Toxicology and Applied Pharmacology 309 (2016) 2–14

Contents lists available at ScienceDirect

Toxicology and Applied Pharmacology

journal homepage: www.elsevier.com/locate/ytaap

Destabilization of mitochondrial functions as a target against breast cancer progression: Role of TPP^+-linked-polyhydroxybenzoates

Cristian Sandoval-Acuña [a,b], Sebastián Fuentes-Retamal [a], Daniela Guzmán-Rivera [a], Liliana Peredo-Silva [a], Matías Madrid-Rojas [c], Solange Rebolledo [c], Vicente Castro-Castillo [d], Mario Pavani [a], Mabel Catalán [a], Juan Diego Maya [a], José A. Jara [e], Eduardo Parra [f], Gloria M. Calaf [g], Hernán Speisky [b], Jorge Ferreira [a,*]

[a] Clinical and Molecular Pharmacology Program, Institute of Biomedical Sciences (ICBM), Faculty of Medicine, University of Chile, Av. Independencia 1027, Santiago 8380453, Chile
[b] Laboratory of Antioxidants, Nutrition and Food Technology Institute, University of Chile, El Líbano 5524, Santiago 7830490, Chile
[c] Department of Chemistry, Faculty of Basic Sciences, Metropolitan Educational Sciences University, Av. José Pedro Alessandri 774, Santiago 7760197, Chile
[d] Department of Organic and Physical Chemistry, Faculty of Chemical and Pharmaceutical Sciences, University of Chile, Santos Dumont 964, Santiago 8380494, Chile
[e] Unit of Pharmacology and Pharmacogenetics, Institute of Dental Sciences Research (ICOD), Faculty of Dentistry, University of Chile, Sergio Livingstone Polhammer 94, Santiago 8380492, Chile
[f] School of Medicine, Faculty of Health Sciences, University of Tarapacá, Av. General Velásquez 1775, Arica 1000007, Chile
[g] Institute for Advanced Research, University of Tarapacá, Antofagasta 1520, Arica 1001236, Chile

ARTICLE INFO

Article history:
Received 8 June 2016
Revised 3 August 2016
Accepted 18 August 2016
Available online 20 August 2016

Keywords:
Human breast cancer
Mitochondrially-targeted decyl polyhydroxybenzoates
Triphenylphosphonium-derivatives
Transmembrane potential
Weak uncoupling of the oxidative phosphorylation system

ABSTRACT

Mitochondrion is an accepted molecular target in cancer treatment since it exhibits a higher transmembrane potential in cancer cells, making it susceptible to be targeted by lipophilic-delocalized cations of triphenylphosphonium (TPP^+). Thus, we evaluated five TPP^+-linked decyl polyhydroxybenzoates as potential cytotoxic agents in several human breast cancer cell lines that differ in estrogen receptor and HER2/neu expression, and in metabolic profile. Results showed that all cell lines tested were sensitive to the cytotoxic action of these compounds. The mechanism underlying the cytotoxicity would be triggered by their weak uncoupling effect on the oxidative phosphorylation system, while having a wider and safer therapeutic range than other uncouplers and a significant lowering in transmembrane potential. Noteworthy, while the TPP^+-derivatives alone led to almost negligible losses of ATP, when these were added in the presence of an AMP-activated protein kinase inhibitor, the levels of ATP fell greatly. Overall, data presented suggest that decyl polyhydroxybenzoates-TPP^+ and its derivatives warrant future investigation as potential anti-tumor agents.

1. Introduction

According to the definition, a group of cells originated in the breast tissue which acquire the ability to avoid growth-inhibiting signals, spread and invade surrounding tissues and metastasizes to distant organs of the body, is called breast cancer (BC) (Unknown, 2014). BC is also a heterogeneous disease with cellular subtypes that have biological distinctness, a different biological behavior, clinical risk factors, natural histories, response to individualized therapy and prognosis. Although a decrease in overall cancer death rates due to a combination of earlier diagnosis and treatment improvement has been recorded, BC remains a worldwide health problem (Gomes et al., 2015); indeed, approximately 70% of patients are inoperable because of an advanced tumor growth or metastasis development (Gomes et al., 2015).

BC is classified into 5 subtypes using the expression of four markers (estrogen receptor (ER), progesterone receptor (PR), human epidermal growth factor receptor-2 (HER2/neu) and Ki-67: (a) luminal A (ER-and/or PR-positive/HER2-negative/low Ki-67), (b) luminal B (ER-and/or PR-positive/HER2-negative/high Ki-67), (c) HER2-positive luminal B (ER-and/or PR-positive/HER2 overexpression/any Ki-67), (d) non-luminal HER2-positive (ER and PR absent/HER2 overexpression), and (e) triple negative breast cancer (TNBC) (ER and PR absent/HER2-negative)(Unknown, 2010; Lamb et al., 2015).

TNBC is the most aggressive subtype, showing a higher rate of distant recurrence and a poorer prognosis than other BC subtypes. Studies have shown that <30% patients with metastatic TNBCs survive up to 5 years and almost all die of this disease due to the absence of effective treatments (Ayub et al., 2015). In order to decrease the incidence, prevalence and worldwide breast cancer death, research must continue to examine new targets that are able to block their growth; as well as

Abbreviations: AMPK, AMP-activated protein kinase; Ap5A, P1,P5-di(adenosine-5′)pentaphosphate; AV, annexin V; BC, breast cancer; BrdU, bromodeoxyuridine; CCCP, carbonyl cyanide m-chlorophenyl hydrazine; CSC, cancer stem cells; ER, estrogen receptor; ETC, electron transport chain; HER2/neu, human epidermal growth factor receptor-2; LDH, lactate dehydrogenase; mtDNA, mitochondrial DNA; $P(Ph)_3$, triphenylphosphine; PI, propidium iodide; PR, progesterone receptor; RFU, relative fluorescence units; ROS, reactive oxygen species; TNBC, triple negative breast cancer; TPP^+, triphenylphosphonium moiety; Ψ_m, mitochondrial transmembrane potential.

* Corresponding author.
E-mail address: jferreir@med.uchile.cl (J. Ferreira).

http://dx.doi.org/10.1016/j.taap.2016.08.018
0041-008X/

to develop more effective chemotherapeutic agents against their malignancy.

Since the last decade, a novel concept has emerged whereby destabilization of mitochondria is a promising effective anti-cancer approach (Fulda et al., 2010; Ralph et al., 2010; Neuzil et al., 2013). In addition to compartmentalizing the metabolic pathways and physiological states of the cell, mitochondria generate a large amount of cellular energy, regulating both the cellular oxidation–reduction (redox) state and the thermogenesis. This energy production is also responsible for an important production of intra-mitochondrial superoxide anion, which is the precursor for most of the cellular reactive oxygen species (ROS), such as hydrogen peroxide, hydroxyl radical or peroxynitrite. It is now clear that cancer cells are found in a restructured metabolic state with increased glycolytic metabolism and continuous use of oxygen even when it is at a very low concentration (close to hypoxia). However, it has been found that ρo tumor cells, which show a depletion of the mitochondrially-coded respiratory complexes with the consequent reduced OXPHOS activity, exhibit an impaired ability to grow and develop metastasis and a dramatic reduction in tumorigenic potential; as well as, being extremely sensitive to cytotoxic drugs (Viale et al., 2015). Electron flow through the respiratory chain process in tumor mitochondria is fundamental, since tumor cells without mitochondrial DNA (mtDNA) showed that tumor formation is associated with acquisition of mtDNA from host cells (mitochondria thieves). This leads to a recovery of mitochondrial functions in cells derived from primary tumors grown from cells without mtDNA; especially, cells from lung metastases exhibited full restoration of respiratory function and no lag in tumor growth. These findings suggest the existence of a horizontal transfer of mtDNA from the host to tumor cells having a compromised mitochondrial function, thus re-establishing respiration and tumor-initiating efficacy. The latter implies the existence of pathophysiological processes to overcome mtDNA damage and support the notion of a high plasticity of malignant cells (Tan et al., 2015; Maiuri and Kroemer, 2015; Villanueva, 2015). Consequently, we consider that tumors depend on the electron flow through the respiratory chain and the consequent generation of the Ψm for the maintenance of their fully transformed phenotype.

A novel concept has emerged whereby destabilization of mitochondria as a target is a promising anti-cancer approach (Fulda et al., 2010). The term “mitocans” has been proposed, referring to molecules with anticancer activity that induce apoptosis by destabilizing mitochondria in cancer cells (Neuzil et al., 2013). Based on their mode of action, mitocans include 8 groups, each comprising of agents with distinct activities, resulting in mitochondrial destabilization and the ensuing induction of the intrinsic apoptotic pathway. Mitocans spread their anti-cancer effect *via* mitochondria; but many of them are hydrophobic compounds that associate with a wide variety of sub-cellular structures and whose uptake by cancer cells may also present a limitation. The best way of increasing their efficiency making them more efficient is to target them directly to mitochondria. We have therefore adapted the approach pioneered by Murphy and Smith (Murphy and Smith, 2007), which consists of tagging antioxidants with the cationic triphenylphosphonium (TPP^+) group. Such an approach increased the lipophilicity of the compounds and targeted these directly to mitochondria, endowing these molecules with enhanced mitochondrial-antioxidant activity when compared to their parent compounds.

Previously, we added the TPP^+ group to the aliphatic chain of several alkyl-gallates, which are the family of antioxidant compounds most commonly used in the processing of food for human consumption and animal industry (Jara et al., 2014). Similarly, we added the TPP^+ group to several mono- and di-OH benzoate decyl ester derivatives. We have also found that lipophilic and delocalized cations of alkyl-gallate derivatives preferentially target mitochondria from cancer cell lines (Jara et al., 2014; Frey et al., 2007). Such TPP^+-derivatives proved to be superior in killing mouse cancer cells, showing IC_{50} values that were 1 to 2 orders of magnitude lower than their respective non-conjugated esters. In addition, TPP^+-conjugates were proven to be considerably less toxic to normal cells. We also found that triphenyl (10-((3,4,5-trihydroxybenzoyl)oxy)decyl) phosphonium bromide (TPP^+C_{10}) induced apoptosis by targeting the mitochondrial inner membrane, resulting in a high oxygen consumption rate and a consequent decrease in Ψ_m and intracellular ATP levels (Jara et al., 2014). Thus, we identified mitochondria as a novel target for anti-cancer activity.

Since the idea of addition of TPP^+ to decyl-polyhydroxybenzoates has been shown to enhance their activity while preserving cancer cell selectivity (exemplified by $C_{10}TPP^+$), we have applied this approach to several other drugs that would belong to a new class of mitocompounds, *i.e.* agents that act by targeting the mitochondrial electron transport chain (ETC), by weakly uncoupling the oxidative phosphorylation system (Lou et al., 2007). Thus, in the present work, we studied the mitochondrially-targeted polyhydroxybenzoates (namely: 2-hydroxy-(SA-TPP^+C_{10}), 2,5-dihydroxy-(GA-TPP^+C_{10}), 2,3-dihydroxy-(PIA-TPP^+C_{10}), 3,4-dihydroxy-(PCA-TPP^+C_{10}) and 3,4,5-trihydroxy-benzoate (TPP^+C_{10})), linked to a triphenylphosphonium moiety (TPP^+) through a ten carbon atom side chain. Their cytotoxic potential against BC cell lines, and a putative mechanism underlying the effect is presented. Results obtained show that the decyl-polyhydroxybenzoates-TPP^+ are cytotoxic for all tested breast cancer cell lines, and that such cytotoxicity could be triggered by their ability to weakly uncouple oxidative phosphorylation. The former event could lead to a loss of mitochondrial potential and, in the long term, to a mild decline in cellular ATP levels. Additionally, the decyl-polyhydroxybenzoates-TPP^+ were shown to inhibit the migratory ability of metastatic BC cells.

2. Materials and methods

2.1. General experimental procedures

The ^1H nuclear magnetic resonance (NMR) spectra was recorded using a Bruker Avance 400 spectrometer equipped with a Bruker inverse 5 mm Z gradient probe operating at 400.13 and 100.62 MHz, respectively. All experiments were conducted at a probe temperature of 300 K using solutions in DMSO-d_6 with tetramethylsilane (TMS) as an internal standard. The chemical shifts are reported as δ (ppm) downfield from TMS for ^1H NMR (spectra shown in supplementary information). Coupling constants (J) are presented in hertz. All compounds meet the criteria of >95% purity, allowing them to show good *in vitro* activity.

2.2. Synthesis of compounds

The synthesis of the decyl-polyhydroxybenzoates-TPP^+ used in the present study (Fig. 1K) was performed in two steps, according to the procedure described in Jara et al. (2014). The first step consisted in the synthesis of (10-hydroxydecyl)triphenylphosphonium bromide performed as follows: a solution of 10-bromodecan-1-ol (277 mg, 1.16 mmol) in dry acetonitrile (100 mL) was treated with triphenylphosphine (310 mg, 1.18 mmol), and the solution was refluxed with stirring at 82 °C for 48 h. Finally, the solvent was removed by a vacuum pump, and the crude product was subjected to chromatography on silica gel (EtOAc, MeOH) to yield (10-hydroxydecyl)triphenylphosphonium bromide as a colorless oil (370 mg, 63%). ^1H NMR (400 MHz, DMSO-d_6): δ 1.01–1.51 (m, 18H, CH_2), 3.57 (t, $J = 7.1$ Hz, 2H, CH_2), 7.73–7.91 (m, 15H, ArH). HRMS: m/z 485.4312 (calculated for $C_{27}H_{33}BrOP$ 485.4357).

The second step involved a Steglich esterification, using *N*,*N*-dicyclohexylcarbodiimide (DCC) as reagent, 4-dimethylaminopyridine (DMAP) as catalyst and *N*,*N*-dimethylformamide (DMF) as solvent. Briefly, in an atmosphere of N_2, a solution of each respective hydroxybenzoic acid (1.3 mmol) in dry DMF (50 mL) was treated with a solution of DCC (272 mg, 1.3 mmol) in dry DMF (30 mL). The mixture was cooled down and kept at 0 °C, and a solution of (10-

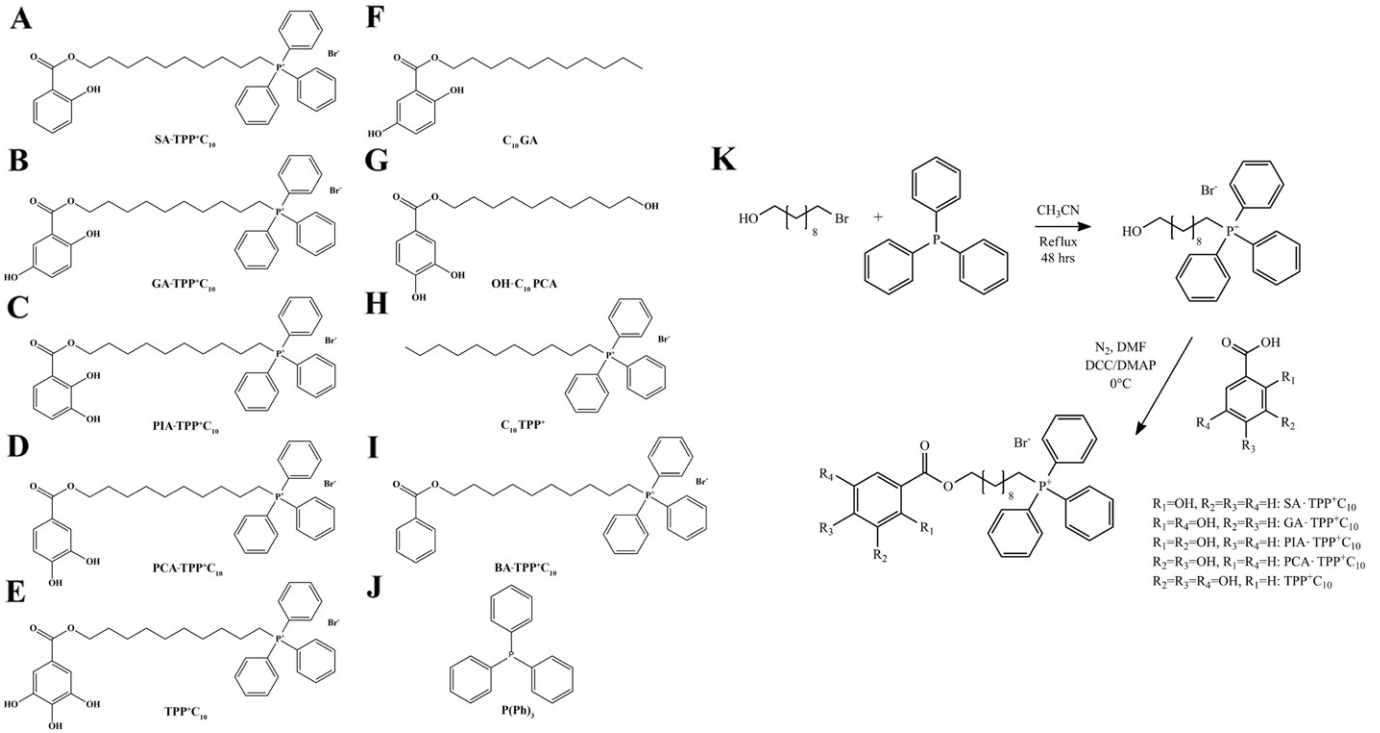

Fig. 1. Structures and synthesis schedule of decyl-polyhydroxybenzoates-TPP^+ and control molecules. The chemical structures of all the decyl-polyhydroxybenzoates-TPP^+ and control molecules used in the present study are depicted, together with the abbreviation used to differentiate them. Structures were obtained using the ChemDraw 9.0 software. (A) (10-((2-hydroxybenzoyl)oxy)decyl)triphenylphosphonium bromide (SA-TPP^+C_{10}), (B) (10-((2,5-dihydroxybenzoyl)oxy)decyl)triphenylphosphonium bromide (GA-TPP^+C_{10}), (C) (10-((2,3-dihydroxybenzoyl)oxy)decyl)triphenylphosphonium bromide (PIA-TPP^+C_{10}), (D) (10-((3,4-dihydroxybenzoyl)oxy)decyl)triphenylphosphonium bromide (PCA-TPP^+C_{10}), (E) triphenyl(10-((3,4,5-trihydroxybenzoyl)oxy)decyl)phosphonium bromide (TPP^+C_{10}), (F) decyl 2,5-dihydroxybenzoate (C_{10}GA), (G) 10-hydroxydecyl 3,4-dihydroxybenzoate (OH C_{10}PCA), (H) decyltriphenylphosphonium bromide (C_{10} TPP^+), (I) (10-(benzoyloxy)decyl)triphenylphosphonium bromide (BA-TPP^+C_{10}), (J) triphenylphosphine (PPh_3). (K) Synthesis schedule of decyl-polyhydroxybenzoates-TPP^+.

hydroxydecyl) triphenylphosphonium bromide (551 mg, 1.1 mmol) in DMF (10 mL) and DMAP (in catalytic amounts) in DMF (5.0 mL) was added. The reaction was stopped the following day, and any resulting precipitate was removed by filtration. The solvent was then removed, producing a residue that was subjected to chromatography on silica gel (DCM, MeOH).

2.2.1. (10-((2-Hydroxybenzoyl)oxy)decyl)triphenylphosphonium bromide (SA-TPP^+C_{10}). Clear yellow oil (41%). ^{1}H NMR (400 MHz, DMSO-d_6): δ 1,13–1,45 (m, 18H, CH_2), 3,35 (t, J = 6,5 Hz, 2H, CH_2), 6,58–6,65 (m, 2H, ArH), 7,13 (t, J = 6,5 Hz, 1H, ArH), 7,73–7,83 (m, 16H, ArH).

2.2.2. (10-((2,5-Dihydroxybenzoyl)oxy)decyl)triphenylphosphonium bromide (GA-TPP^+C_{10}). Dark brown oil (70%). ^{1}H NMR (400 MHz, DMSO-d_6): δ 1,10–1,50 (m, 18H, CH_2), 3,34 (t, J = 6,5 Hz, 2H, CH_2), 6,50 (d, J = 8,6 Hz, 1H, ArH), 6,68 (dd, J = 8,5 Hz, J = 2,7 Hz, 1H, ArH), 7,20 (d, J = 2,5 Hz, 1H, ArH) 7,70–7,95 (m, 15H, ArH).

2.2.3. (10-((2,3-Dihydroxybenzoyl)oxy)decyl)triphenylphosphonium bromide (PIA-TPP^+C_{10}). Dark yellow oil (39%). ^{1}H NMR (400 MHz, DMSO-d_6): δ 1,16–1,48 (m, 18H, CH_2), 3,36 (t, J = 6,1 Hz, 2H, CH_2), 6,37 (t, J = 7,6 Hz, 1H, ArH), 6,69 (d, J = 7,4 Hz, 1H, ArH), 7,16 (d, J = 7,5 Hz, 1H, ArH), 7,72–7,92 (m, 15H, ArH).

2.2.4. (10-((3,4-Dihydroxybenzoyl)oxy)decyl)triphenylphosphonium bromide (PCA-TPP^+C_{10}). Clear yellow oil (76%). ^{1}H NMR (400 MHz, DMSO-d_6): δ 1,14–1,47 (m, 18H, CH_2), 3,35 (t, J = 6,5 Hz, 2H, CH_2), 6,74 (d, J = 8,2 Hz, 1H, ArH), 7,27 (d, J = 8,0 Hz, 1H, ArH), 7,35 (s, 1H, ArH) 7,76–7,94 (m, 15H, ArH).

2.2.5. Triphenyl(10-((3,4,5-trihydroxybenzoyl)oxy)decyl)phosphonium bromide (TPP^+C_{10}). Dark yellow oil (72%). ^{1}H NMR (400 MHz, DMSO-d_6): δ 1,18–1,52 (m, 18H, CH_2), 3,43 (t, J = 6,3 Hz, 2H, CH_2), 7,72–7,92 (m, 17H, ArH).

2.3. Cell lines and cell culture

Human breast cancer cell lines MCF7 (ATCC® code HTB-22™, ER^+-HER2/neu^-), AU565 (ATCC® code CRL-2351™, ER^--HER2/neu^+), BT-549 (ATCC® code HTB-122™, ER^--HER2/neu^-), MDA-MB-361 (ATCC® code HTB-27™, ER^+-HER2/neu^+) and MDA-MB-231 (ATCC® code HTB-26™, ER^--HER2/neu^-), and the normal breast-epithelial cell line MCF 10F (ATCC® code CRL-10318™), were all purchased from ATCC (ATCC, Manassas, VA, USA). All cells were used within 6 months of their initial defrosting and cultured as instructed by ATCC.

2.4. Cellular viability

The evaluation of the effect of the molecules studied (0.1–100 μM) on the viability of all five breast cancer cell lines was performed by the MTT reduction assay (Detailed methodology is provided in S.I.). IC_{50} values for each condition were calculated by interpolating in a dose-response curve and are expressed as mean ± SEM. Additionally, LDH release induced by C_{10}GA, GA-TPP^+C_{10} or $C_{10}TPP^+$ (10 and 20 μM) was measured in MCF7 and MDA-MB-231 cells using the LDH-Cytotoxicity Assay Kit II (Abcam, Cambridge, UK; a detailed methodology is provided in S.I.). All values are expressed as percentage of LDH activity relative to cells incubated with Cell Lysis solution (provided in the kit) for 24 h.

2.5. Oxygen consumption

The effect on cellular oxygen consumption of the compounds studied (10, 20 and 50 μM) was determined in MCF7 and MDA-MB-231 cells by means of a Clark-type electrode (Yellow Springs Instruments, Yellow Spring, OH, USA) as described in S.I. Results are expressed as the ratio between the oxygen consumption rate (OCR) previously inhibited by oligomycin and after the addition of the uncoupling agent (CCCP or the studied compounds).

2.6. Mitochondrial superoxide anion levels

Superoxide anion production induced by all five decyl-polyhydroxybenzoates-TPP^+ (2.5–50 μM) was determined in MCF7 and MDA-MB-231 cells by flow cytometry (FACSAria®III, BD Biosciences), using the fluorescent probe MitoSOX Red® as described in S.I. Control corresponds to MitoSOX-loaded cells incubated only with PBS, and results are expressed as percentage of relative fluorescence units (RFU) over control.

2.7. Mitochondrial membrane potential

The effect of decyl-polyhydroxybenzoates-TPP^+ (5, 10 and 20 μM) on mitochondrial membrane potential (Ψ_m) was assessed in MCF7 and MDA-MB-231 cells by means of the fluorescent probe safranin-O (Detailed methodology is presented in S.I.). Total Ψ_m loss was attained in a separate measurement by adding CCCP (0.5 μM).

2.8. Cellular ATP levels

The effect of the studied compounds (2.5–20 μM) on cellular ATP was measured in MCF7, MDA-MB-231 and MCF 10F cells using the CellTiter-Glo® Luminescent Cell Viability Assay kit (Promega, Madison, WI, USA), as described in S.I. A similar experiment was performed incubating cells with 10 and 20 μM of GA-TPP^+ C_{10} and PCA-TPP^+ C_{10} in the presence of either Compound C (1 μM) or Ap5A (5 μM). All results are expressed as percentage of ATP relative to control cells treated only with vehicle.

2.9. Annexin V/propidium iodide staining

The type of cell death induced by the compounds (at concentrations of 2.5–5 μM for MCF7 and MCF 10F cells and 10–20 μM for MDA-MB-231 cells) was assessed by flow cytometry (FACSAria®III), using annexin V/propidium iodide (AV/PI) double staining, following the instructions of the Annexin V-FITC Apoptosis Detection Kit (Abcam; detailed methodology provided in S.I.). Results are expressed as total apoptotic cells (percentage of AV+/PI− and AV+/PI+ cells) and live cells (percentage of AV−/PI− cells).

2.10. Cellular migration (wound healing assay)

The effect of GA-TPP^+ C_{10} and PCA-TPP^+ C_{10} (1, 2.5 y 5 μM) on the migration of MDA-MB-231 cells was assessed by means of the wound healing assay, as described in S.I. Results are expressed as % wound area compared to t0.

2.11. Statistics

Results are expressed as mean ± SEM of at least three independent experiments. Normality of all data was tested by Shapiro-Wilk normality test. The comparison between experimental groups and control was performed by one- or two-way ANOVA with Bonferroni post-test, using the GraphPad Prism 5.0 software. $p < 0.05$ was established as the minimum significance level.

3. Results

3.1. Synthesis of delocalized lipophilic cations derivatives

The synthetic route (see Section 2.2) allowed us to derive a series of decyl-polyhydroxybenzoates linked to TPP^+ that differed in the number and position of the hydroxyl groups on the benzoic acid ring (Fig. 1A–E).

3.2. Cellular viability

Results showed that GA-TPP^+ C_{10} reduced cell viability in a dose-dependent manner in the five cell lines (Fig.2). Furthermore, the effect of this compound also showed a slight time-dependency in the case of MDA-MB-361 (Fig. 2A), MCF7 (Fig. 2B), AU565 (Fig. 2C) and BT-549 (Fig. 2D) cell lines, since the dose-response curves were shifted to lower concentrations at 48 and 72 h of incubation. However, the cell line MDA-MB-231 (Fig. 2E) showed a lower effect on the cytotoxicity induced, as observed in the three curves obtained. The same experiment was performed with each of the other decyl-polyhydroxybenzoates-TPP^+ under study. The respective dose-response curves obtained showed similar results in terms of the concentration-dependence of their cytotoxic effects (Table I). It is noted that IC_{50} values for the decyl-polyhydroxybenzoates-TPP^+ at 24 h of incubation are relatively similar between all compounds and cell lines, ranging from 6 to 15 μM (Table I). Nonetheless, while the four former cell lines evidenced a marked decrease in the IC_{50} values at 48 and 72 h, showing a range of between 2 and 5 μM and between 1 and 3 μM, respectively, the MDA-MB-231 cell line showed a minor shift in the IC_{50} values, with values of 10–13 μM, 8–12 μM, and 7–9 μM after 24, 48 and72 h of incubation, respectively (Table I).

Similarly, Table II includes IC_{50} values obtained after incubating MCF7, AU565 and MDA-MB-231 cells with each of the control molecules for 24, 48 and 72 hours. Results showed that, both C_{10}GA and OH-C_{10}PCA had almost no cytotoxic effect at concentrations up to 400 μM, and $P(Ph)_3$ has IC_{50} values between 10- and 40-fold higher than those exhibited by the decyl-polyhydroxybenzoates-TPP^+ in all cell lines. Also, the BA-TPP^+ C_{10} showed no toxicity in concentrations up to 50 μM (Table II). However, the $C_{10}TPP^+$ molecule exerted a mild cytotoxic activity at 24 h in all cell lines tested, with IC_{50} values ranging between 2 and 33 μM, and a significantly enhanced cytotoxicity after 48 and 72 h, reaching values of 0.5–7 μM and 0.1–3 μM, respectively (Table II).

Given the similarity of the cytotoxic effect of the decyl-polyhydroxybenzoates-TPP^+ in the breast cancer cell lines MDA-MB-361, MCF7, AU565 and BT-549 (Fig. 2 and Table I), and the slight difference shown by the MDA-MB-231 cells, we decided to continue the study of the putative mechanism underlying such toxicity using only MCF7 and MDA-MB-231 cells.

In order to address the type of cytotoxicity elicited by each class of compound (decyl-polyhydroxybenzoates-TPP^+, non-TPP^+ decyl-polyhydroxybenzoates and decyl-TPP^+), MCF7 and MDA-MB-231 cells were incubated with two concentrations (10 and 20 μM) of GA-TPP^+ C_{10}, C_{10}GA or $C_{10}TPP^+$ for 24 h, and the LDH leakage was measured. As depicted in Fig. S1, while cells treated with GA-TPP^+ C_{10} and C_{10}GA showed only a minor LDH release (around 5% relative to control), cells treated with $C_{10}TPP^+$ showed a much greater LDH leakage (>50% relative to control).

3.3. Oxygen consumption

In order shed light on the mechanism that might underlie the cytotoxicity exerted by the decyl-polyhydroxybenzoates-TPP^+, cellular oxygen consumption after the addition of each compound was measured. Data showed that while MCF7 cells seem to have a higher rate of basal oxygen consumption, MDA-MB-231 cells are almost not affected by the complex V inhibitor oligomycin. The latter might be explained by

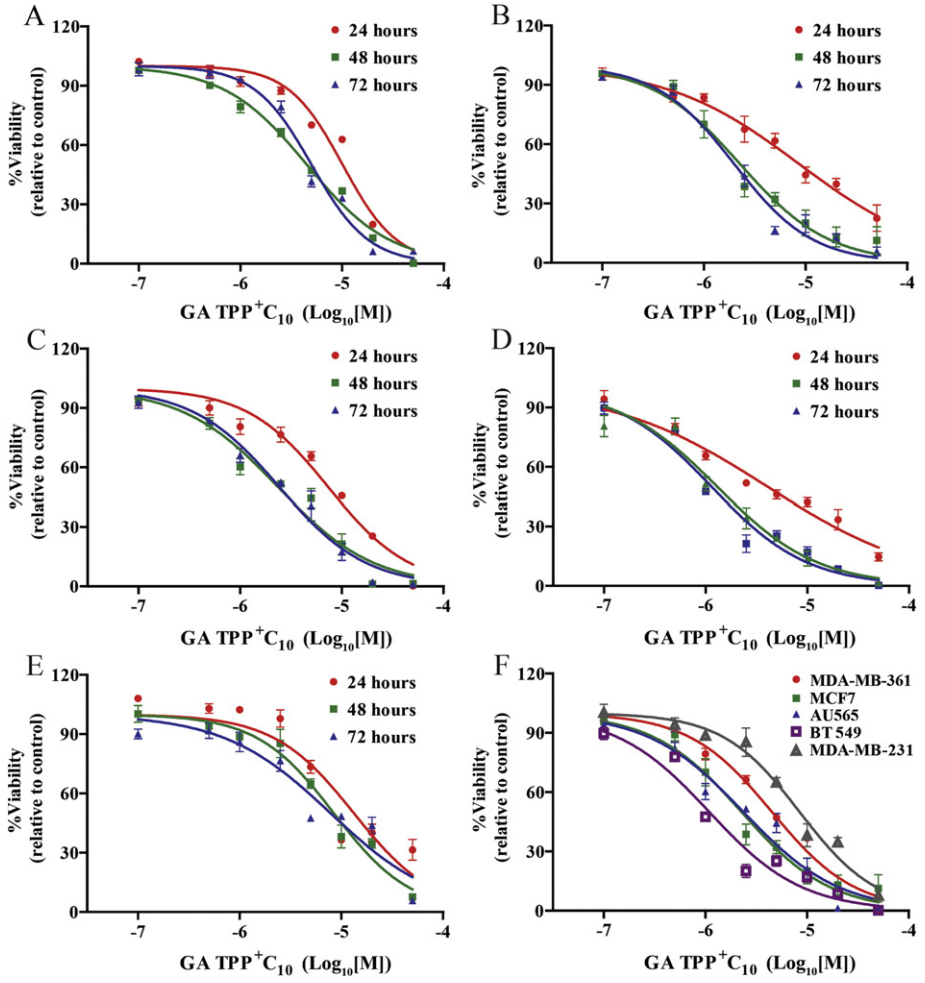

Fig. 2. Cytotoxic activity of TPP^+ linked-gentisic acid in different breast cancer cell lines. Human breast cancer cell lines (A) MDA-MB-361, (B) MCF7, (C) AU565, (D) BT-549 and (E) MDA-MB-231, were incubated with increasing concentrations of GA-TPP^+C_{10} (0.1–50 μM) for 24, 48 and 72 h. Viability was assessed by the MTT reduction assay, as described in Material and methods. (F) Comparison of viability curves for the incubation of each cell line with GA-TPP^+C_{10} (0.1–50 μM) for 48 h. The % of viability was calculated as the reduction of MTT (read as $\lambda_{570\ nm}$) relative to that observed in cells incubated only with vehicle. Values are expressed as mean ± SEM (n = 3) and semi-logarithmic dose-response curves were obtained using the GraphPad Prism software (version 5).

the higher presence of the complex V endogenous-inhibitor IF1, which could also underlie their decreased respiration, due to the inhibition of ATP synthesis (Sanchez-Arago et al., 2013; Barbato et al., 2015; Sanchez-Cenizo et al., 2010; Sanchez-Arago et al., 2012) (Fig. 3A and E). Such observation is in agreement with the fact that MDA-MB-231 cells depolarized with rotenone (10 μM) do not undergo repolarization after the addition of ATP, implying that their Complex V ATPase-activity is strongly inhibited, while MCF7 cells do increase their rotenone-diminished transmembrane potential after the addition of ATP (Fig. S3). Nonetheless, all compounds increased, concentration-dependently, cellular oxygen consumption, relative to the oligomycin-inhibited respiration, in both cell lines (Figs. 3 and S2). It is important to mention that although MDA-MB-231 cells exhibited a higher level of maximal oxygen consumption after the addition of CCCP (0.5 μM) than that shown by MCF7 cells (Figs. 3 and S2), the highest concentration of the decyl-polyhydroxybenzoates-TPP^+ exerted the same level of increase in oxygen consumption as did the classic uncoupler in both cases.

3.4. Mitochondrial superoxide anion production

Subsequently, the level of mitochondrial superoxide anion was measured. As shown, concentrations of up to 10 μM of the decyl-polyhydroxybenzoates-TPP^+ had no effect on mitochondrial superoxide anion levels in both MCF7 and MDA-MB-231 cells. In the former cell line, concentrations of 20 μM of each compound increased only slightly the superoxide anion production (Fig. S4), while in MDA-MB-231 cells such production was increased up to 2–3.5-fold relative to control (Fig. S5). Similarly, when concentrations of 50 μM were added, superoxide anion levels were increased by almost 2 fold in MCF7 cells and by approximately 4-fold in MDA-MB-231.

3.5. Mitochondrial transmembrane potential

The effect of increasing concentrations of the decyl-polyhydroxybenzoates-TPP^+ (5, 10 and 20 μM) on mitochondrial membrane potential in MCF7 and MDA-MB-231 cells was assessed by means of the fluorescent probe safranin-O (Figs. 4 and S6). All compounds tested are able to concentration-dependently induce the loss of Ψ_m, as evidenced by the increasing slope of the RFU *vs.* time curves at higher concentrations. Furthermore, when the compounds were added at 20 μM, the loss of Ψ_m was almost equal to that observed after the addition of CCCP (0.5 μM). Interestingly, in contrast with what was observed in Fig. 3, no difference was evident between the effect of CCCP in MCF7 and MDA-MB-231 cells. The quantification of the effect of decyl-polyhydroxybenzoates-TPP^+ on mitochondrial membrane potential was performed by analyzing the area under the curve (AUC) for each condition. Results showed no difference between the effects of the five compounds in the two cell lines used. Thus, AUC for 20 μM of all compounds was 95% ± 2.5% of that obtained for CCCP 0.5 μM (not-significant). In turn, AUC for 10 μM and 5 μM of all compounds were 80% ±

Table I
IC50 values for decyl-polyhydroxybenzoates-TPP$^+$ in all cell lines.

Compound	24 h	48 h	72 h
A. MDA-MB-361 [μM]			
SA-TPP$^+$C$_{10}$			
GA-TPP$^+$C$_{10}$	13.53 ± 0.72	5.69 ± 0.48[a]	3.93 ± 0.45[a,b]
PIA-TPP$^+$C$_{10}$			
PCA-TPP$^+$C$_{10}$	16.44 ± 1.1	4.75 ± 0.43[a]	2.96 ± 0.37[a,b]
TPP$^+$C$_{10}$			
B. MCF7 [μM]			
SA-TPP$^+$C$_{10}$	13.96 ± 0.53	2.33 ± 0.18[a]	2.35 ± 0.32[a]
GA-TPP$^+$C$_{10}$	9.41 ± 1.05	2.35 ± 0.43[a]	2.34 ± 0.12[a]
PIA-TPP$^+$C$_{10}$	12.12 ± 2.00	5.17 ± 0.51[a]	3.14 ± 0.21[a,b]
PCA-TPP$^+$C$_{10}$	11.54 ± 0.83	3.72 ± 0.48[a]	2.03 ± 0.50[a]
TPP$^+$C$_{10}$	14.4 ± 0.78	6.17 ± 0.48[a]	3.33 ± 0.20[a,b]
C. AU565 [μM]			
SA-TPP$^+$C$_{10}$	9.39 ± 0.37	2.88 ± 0.21[a]	2.75 ± 0.32[a]
GA-TPP$^+$C$_{10}$	12.43 ± 1.39	3.44 ± 0.61[a]	3.20 ± 0.31[a]
PIA-TPP$^+$C$_{10}$	13.85 ± 2.96	3.05 ± 0.14[a]	3.27 ± 0.19[a]
PCA-TPP$^+$C$_{10}$	11.41 ± 1.04	2.70 ± 0.47[a]	1.68 ± 0.52[a]
TPP$^+$C$_{10}$	13.71 ± 2.70	5.01 ± 0.06[a]	2.25 ± 0.07[a,b]
D. BT-549 [μM]			
SA-TPP$^+$C$_{10}$	6.45 ± 1.88	1.67 ± 0.57[a]	1.89 ± 0.86[a]
GA-TPP$^+$C$_{10}$	4.82 ± 0.41	1.20 ± 0.10[a]	1.48 ± 0.24[a]
PIA-TPP$^+$C$_{10}$	7.04 ± 0.45	2.40 ± 0.20[a]	1.51 ± 0.02[a]
PCA-TPP$^+$C$_{10}$	5.31 ± 0.67	1.59 ± 0.35[a]	1.60 ± 0.18[a]
TPP$^+$C$_{10}$	6.04 ± 1.84	5.04 ± 1.08	2.52 ± 0.78[a,b]
E. MDA-MB-231 [μM]			
SA-TPP$^+$C$_{10}$	13.77 ± 0.52	8.34 ± 1.00	7.25 ± 0.18[a]
GA-TPP$^+$C$_{10}$	10.08 ± 0.42	8.01 ± 0.57	7.23 ± 0.15
PIA-TPP$^+$C$_{10}$	12.65 ± 1.57	9.86 ± 0.30	9.0 ± 1.1
PCA-TPP$^+$C$_{10}$	14.62 ± 0.73	10.63 ± 0.45	8.03 ± 0.37[a]
TPP$^+$C$_{10}$	13.31 ± 1.56	11.99 ± 0.17	7.77 ± 0.50[a,b]

IC_{50} values (in μM) were calculated from sigmoidal dose-response curves obtained from MTT reduction assays. Each value represents the mean of at least three independent experiments performed in triplicate (mean ± SEM).

[a] Significant difference compared to same cell line and compound after 24 h (two way ANOVA with Bonferroni post-test; $p < 0.05$).

[b] significant difference compared to same cell line and compound after 48 h (two way ANOVA with Bonferroni post-test; $p < 0.05$).

Table II
IC_{50} values for control molecules in MCF7, AU565 and MDA-MB-231 cells.

Compound	24 h	48 h	72 h
A. MCF7 [μM]			
C$_{10}$GA	>400	>400	>400
OH-C$_{10}$PCA	>400	>400	>400
C$_{10}$TPP$^+$	33.1 ± 1.6	7.4 ± 1.4[a]	0.4 ± 0.1[a,b]
BA-TPP$^+$C$_{10}$	>50	>50	>50
Gallic acid	364.73 ± 6.64	292.73 ± 6.81[a]	183.90 ± 7.42[a,b]
P(Ph)$_3$	75.89 ± 1.33	72.08 ± 2.12	73.05 ± 0.94
B. AU565 [μM]			
C$_{10}$GA	>400	>400	>400
OH-C$_{10}$PCA	>400	>400	>400
C$_{10}$TPP$^+$	2.15 ± 0.39	0.57 ± 0.01[a]	0.39 ± 0.02[a]
BA-TPP$^+$C$_{10}$	>50	>50	>50
Gallic acid	99.15 ± 3,99	73.33 ± 4.01[a]	74.57 ± 3.83[a]
P(Ph)$_3$	109.03 ± 3.16	95.20 ± 2.36	92.60 ± 2.23
C. MDA-MB-231 [μM]			
C$_{10}$GA	>400	>400	>400
OH-C$_{10}$PCA	>400	>400	>400
C$_{10}$TPP$^+$	3.0 ± 1.1	0.7 ± 0.1[a]	0.1 ± 0.07[a]
BA-TPP$^+$C$_{10}$	>50	>50	>50
Gallic acid	373.80 ± 9.96	336.33 ± 9.59[a]	340.57 ± 14.87[a]
P(Ph)$_3$	202.03 ± 11.00	205.77 ± 5.57	210.3 ± 6.29

IC_{50} values (in μM) were calculated from sigmoidal dose-response curves obtained from MTT reduction assays. Each value represents the mean of at least three independent experiments preformed in triplicate (mean ± SEM).

[a] Significant difference compared to same cell line and compound after 24 h (two way ANOVA with Bonferroni post-test; $p < 0.05$).

[b] Significant difference compared to same cell line and compound after 48 h (two way ANOVA with Bonferroni post-test; $p < 0.05$).

1.4% and 71% ± 2.4%, respectively (both significantly different from CCCP; $p < 0.05$).

3.6. ATP levels

We thereafter assessed the effect of the decyl-polyhydroxybenzoates-TPP$^+$ (at 2.5, 5, 10 and 20 μM) on the total ATP levels of MCF7 and MDA-MB-231 cells. As shown in Fig. S7, the compounds had a minor effect on the ATP levels of MCF7 cells, lowering these only to near 75% of control levels at the highest concentration used (20 μM). In MDA-MB-231 cells the effect of the decyl-polyhydroxybenzoates-TPP$^+$ was even lower, with the highest concentration of each compound tested, lowering the ATP levels by only about 10% (Fig. S8).

Several intracellular metabolic sensors are activated when the ATP/ADP ratio falls, rendering the cells able to cope with a diminished ATP production by the activation of several pathways of ATP synthesis and the inactivation of ATP consuming processes (Yuan et al., 2013). Thus, the activation of AMPK after the addition of the decyl-polyhydroxybenzoates-TPP$^+$ to cells might increase non-mitochondrial ATP synthesis, allowing cells to cope with the expected decrease in ATP levels induced by such compounds. In order to test the latter hypothesis, ATP levels of MCF7 and MDA-MB-231 cells were incubated with GA-TPP$^+$C$_{10}$ and PCA-TPP$^+$C$_{10}$ (at 10 and 20 μM), in the absence or presence of the AMPK inhibitor Compound C (Ma et al., 2014) (1 μM) were measured (Fig. 5). As shown, the sole addition of Compound C had no effect on ATP level. Nonetheless, its addition to decyl-polyhydroxybenzoate-TPP$^+$-treated MCF7 cells resulted in a higher fall of cellular ATP, reaching about 57% at 10 μM and 35% at 20 μM of decyl-polyhydroxybenzoates-TPP$^+$ (compared to 85% and 75%, respectively, in the absence of Compound C) (Fig. 5A, black bars). Similarly, MDA-MB-231 cells co-incubated with Compound C and decyl-polyhydroxybenzoates-TPP$^+$ showed a decrease in their ATP levels compared to cells incubated only with decyl-polyhydroxybenzoates-TPP$^+$, although such decrease was less marked than in MCF7 cells, reaching about 85% and 75% at 10 and 20 μM, respectively (compared to 97% and 85% in the absence of Compound C; Fig. 5B, black bars).

Another important metabolic sensor is adenylate kinase (Dzeja and Terzic, 2009). Thus, we assessed the effect of the adenylate kinase inhibitor Ap5A (Kurebayashi et al., 1980) (5 μM), on ATP levels of MCF7 and MDA-MB-231 cells co-incubated with GA-TPP$^+$C$_{10}$ and PCA-TPP$^+$C$_{10}$ (at 10 and 20 μM). Results show that while Ap5A by itself has no effect in the cellular ATP, when MCF7 cells were co-incubated with Ap5A and the decyl-polyhydroxybenzoates-TPP$^+$, ATP levels were reduced significantly, falling from 85% and 75% at 10 and 20 μM decyl-polyhydroxybenzoates-TPP$^+$, respectively, to near 71% and 55% in the presence of Ap5A (Fig. 5A, grey bars). In MDA-MB-231 cells the effect was less marked, with Ap5A inducing a reduction of ATP levels in decyl-polyhydroxybenzoates-TPP$^+$-treated cells from 93% and 90%, to near 89% and 81% at 10 and 20 μM, respectively at the incubation times used in these assays (Fig. 5B, grey bars). Of particular note, ATP levels of normal breast epithelia cell line MCF 10F were not significantly affected by decyl-polyhydroxybenzoates-TPP$^+$, either alone or in combination with Compound C or Ap5A (Fig. 5C).

3.7. Apoptosis induction

In order to determine the type of death induced by the compounds, double staining with Annexin V-FITC and propidium iodide was used. Results show that both GA-TPP$^+$C$_{10}$ and PCA-TPP$^+$C$_{10}$ (at 2.5 and 5 μM) are able to significantly induce apoptosis in MCF7 cells after a 48-hour incubation, reaching almost 55% at the higher concentration (Fig. 6A and B). In contrast, MDA-MB-231 showed a lower response to

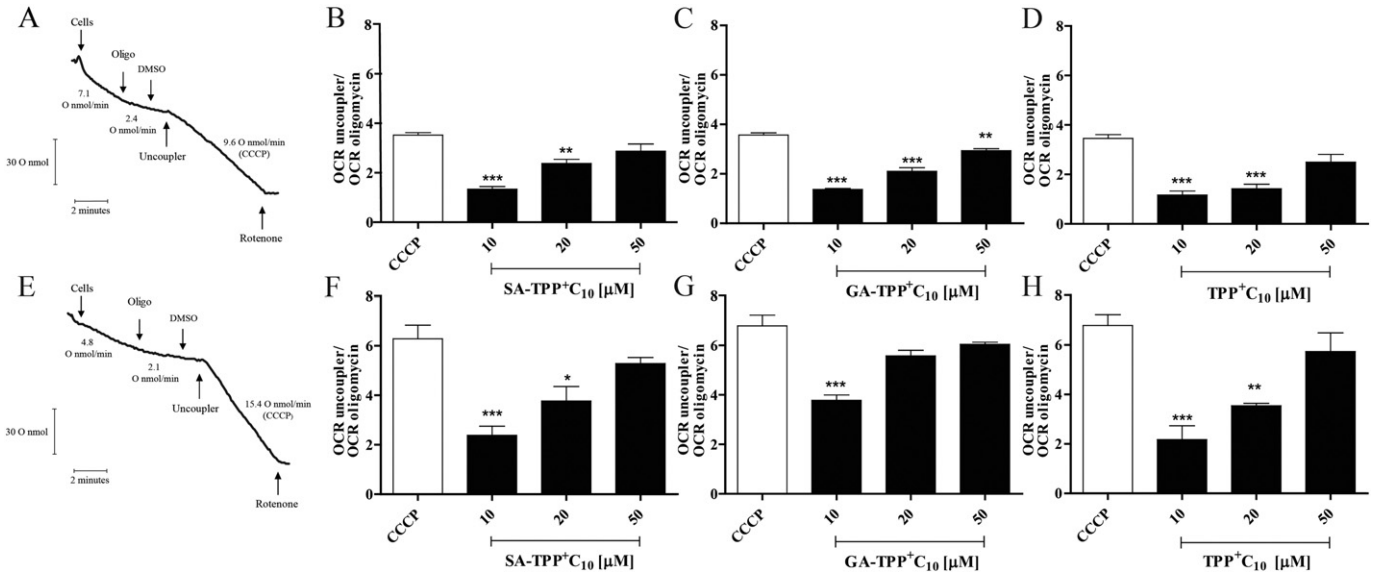

Fig. 3. Oxygen consumption of cells treated with decyl-polyhydroxybenzoates-TPP$^+$. (A) Schematic representation of the oxygen consumption assay in MCF7 cells. MCF7 cells, pre-incubated with oligomycin (2.5 μg/mL), were added increasing concentrations (10, 20 or 50 μM) of (B) SA-TPP$^+$C$_{10}$, (C) GA-TPP$^+$C$_{10}$ or (D) TPP$^+$C$_{10}$ and oxygen consumption rate was measured by means of a Clark electrode. (E) Schematic representation of the oxygen consumption assay in MDA-MB-231 cells. MDA-MB-231 cells, previously added oligomycin (2.5 μg/mL), were added increasing concentrations (10, 20 or 50 μM) of (F) SA-TPP$^+$C$_{10}$, (G) GA-TPP$^+$C$_{10}$ or (H) TPP$^+$C$_{10}$ and oxygen consumption rate was measured by means of a Clark electrode. (A) and (E) include the oxygen consumption rates of each respiratory state (basal, oligomycin-inhibited and CCCP-uncoupled). Results in (B–D) and (F–H) are expressed as the ratio between oxygen consumption rate after and before the addition of the TPP$^+$-polyhydroxybenzoates (mean ± SEM, n = 3). CCCP (0.5 μM) was used as a positive uncoupling control. *: significant difference compared to CCCP (one way ANOVA with Bonferroni post-test; $p < 0.05$), **: $p < 0.01$, ***: $p < 0.001$.

the apoptotic action of both compounds, even when 4-fold higher concentrations were used (10 and 20 μM for 48 h). Indeed, 20 μM of decyl-polyhydroxybenzoates-TPP$^+$ only induced around 35% apoptotic death (Fig6C and D). Interestingly, GA-TPP$^+$C$_{10}$ and PCA-TPP$^+$C$_{10}$ had a lower effect in normal breast epithelial cells MCF 10F. When added at similar concentrations as in MCF7 cells, both induced only 10% and 25% of death (at 2.5 and 5 μM, respectively; Fig. 6E and F).

3.8. Cellular migration

The effect on the migratory ability of MDA-MB-231 was assayed by means of the wound-healing assay. Fig. 7A shows the images obtained from cells incubated with GA-TPP$^+$C$_{10}$ and PCA-TPP$^+$C$_{10}$ (5 μM) for 0–72 h after the wound. While cells incubated with BrdU or DMSO closed the wound area up to a 99% and 65%, respectively, the decyl-

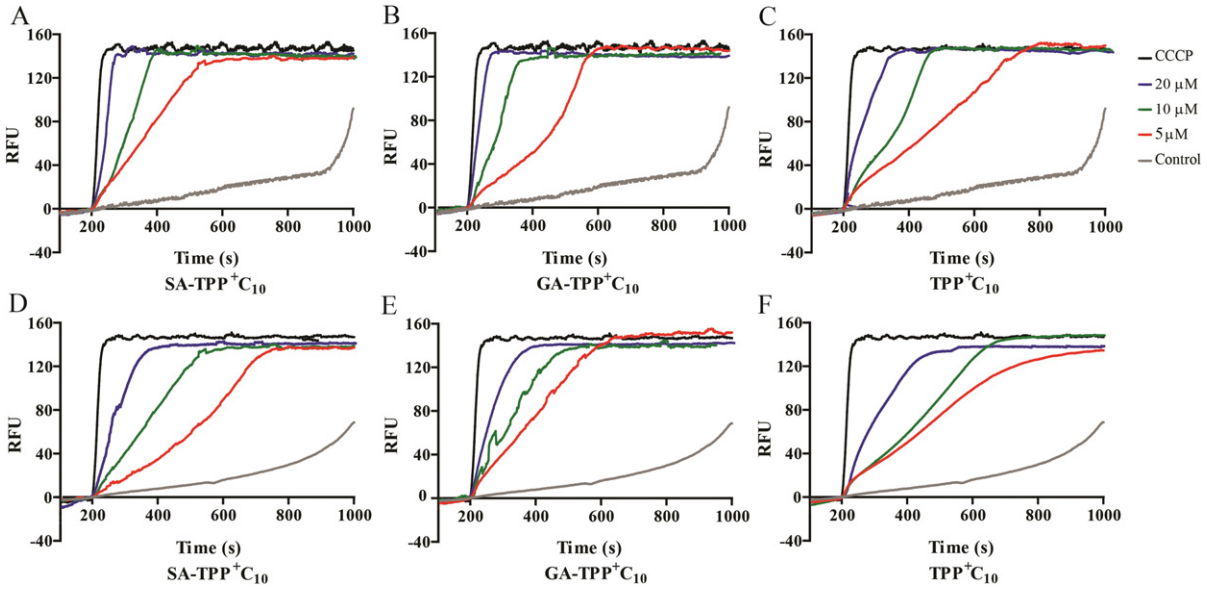

Fig. 4. Mitochondrial membrane potential of cells treated with decyl-polyhydroxybenzoates-TPP$^+$. MCF7 human breast cancer, pre-incubated with glutamate/malate, digitonin and safranin-O for 10 min were added increasing concentrations (5, 10 or 20 μM) of (A) SA-TPP$^+$C$_{10}$, (B) GA-TPP$^+$C$_{10}$ or (C) TPP$^+$C$_{10}$. MDA-MB-231 human breast cancer, pre-incubated with glutamate/malate, digitonin and safranin-O for 10 min were added increasing concentrations (5, 10 or 20 μM) of (D) SA-TPP$^+$C$_{10}$, (E) GA-TPP$^+$C$_{10}$ or (F) TPP$^+$C$_{10}$. Safranin-O fluorescence was recorded for 200 s prior and 800 s after the addition of the TPP$^+$-derivatives. Curves depict safranin-O relative fluorescence units *versus* time. CCCP (0.5 μM) was used as a positive uncoupling control. Each curve represents the mean of at least three independent experiments.

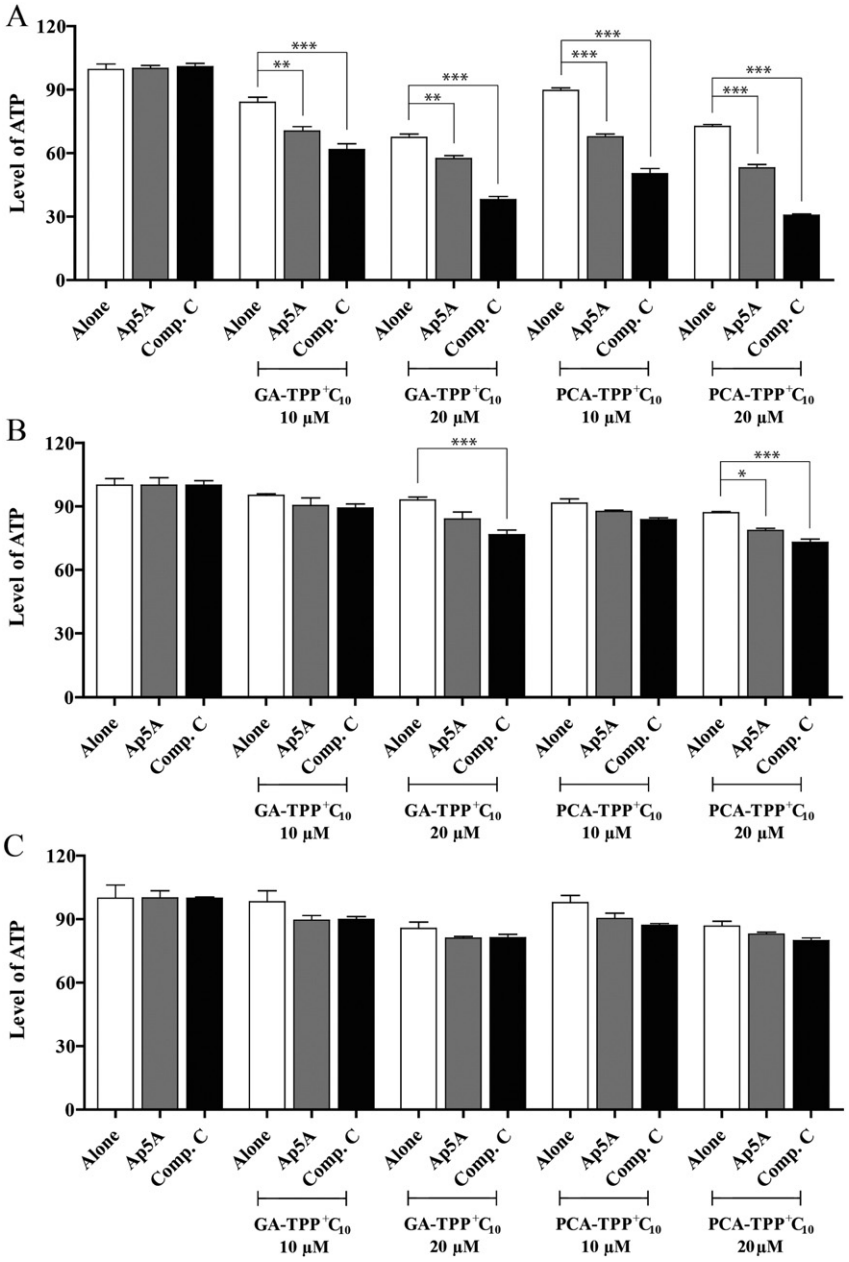

Fig. 5. Effect of metabolic inhibitors on ATP levels of MCF7, MDA-MB-231 and MCF 10F cells incubated with decyl-polyhydroxybenzoates-TPP^+. (A) MCF7 human breast cancer cells, (B) MDA-MB-231 human breast cancer cells and (C) MCF 10F human normal breast epithelial cells were incubated during 4 h with 10 or 20 μM of either GA-TPP^+C_{10} or PCA-TPP^+C_{10}. Incubations were done in the absence (white bars) or presence of either the AMPK inhibitor Compound C (1 μM, during the 4 h, black bars) or the adenylate kinase inhibitor Ap5A (5 μM, during the last hour, grey bars). Intracellular ATP levels were assessed by means of the CellTiter-Glo® Luminescent Cell Viability Assay kit (Promega). Control columns represent cells incubated only with vehicle in the absence or presence of the inhibitors and the results are expressed as percentage of each respective control (mean ± SEM, n = 3). *: significant difference compared to same concentration of TPP^+-derivative in the absence of inhibitors (two way ANOVA with Bonferroni post-test; $p < 0.05$), **: $p < 0.01$, ***: $p < 0.001$.

polyhydroxybenzoate-TPP^+-incubated cells only showed a 30% of wound closing at the highest concentration used (Fig. 7B and C). Such inhibitory effect appears to be concentration-dependent, since lower concentrations allowed a more effective wound closing (near 55% and 45% at 1 and 2.5 μM, respectively).

4. Discussion

The need of developing new treatments for breast cancer has driven considerable investigation around new compounds that could be targeted directly to mitochondria, interfering with cancer cells metabolism (Ralph et al., 2010; Yan et al., 2015). Based on our previous findings on the ability of a 3,4,5-trihydroxy-benzoate triphenylphosphonium-derivative to selectively eliminate mouse breast cancer cells (Jara et al., 2014; Frey et al., 2007), in the present study we modified four additional decyl-benzoates with the TPP^+ moiety, in order to compare their cytotoxic potential in a panel of five different human breast cancer cell lines. The basis of the mitochondrial targeting of TPP^+-linked molecules lies on the attraction that the negatively charged inner face of the inner mitochondrial membrane exerts over cations (Modica-Napolitano and Aprille, 2001; Madak and Neamati, 2015). Despite its charge, TPP^+ cations can easily cross biological membranes due to both their lipophilicity and their ability to delocalize the positive charge between their three aromatic rings (Madak and Neamati, 2015). Moreover, since the mitochondria of cancer cells have been shown to possess a significantly higher Ψ_m, the mitochondrial targeting of cytotoxic compounds with TPP^+ cations could represent a significant improvement of the selectivity of the linked molecules (Modica-Napolitano and Aprille, 2001).

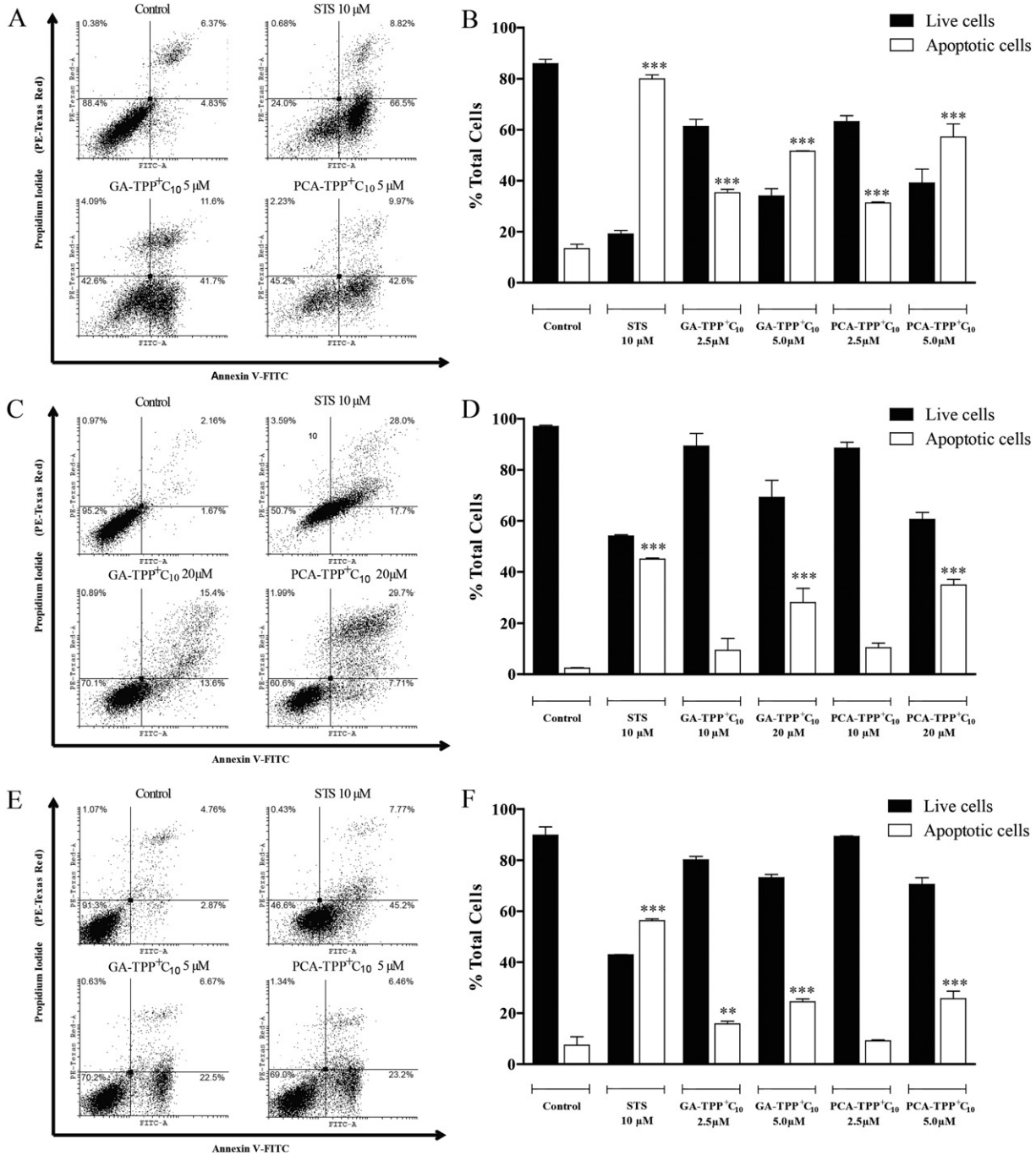

Fig. 6. Apoptosis induction on MCF7, MDA-MB-231 and MCF 10F cells incubated with decyl-polyhydroxybenzoates-TPP$^+$. MCF7 human breast cancer cells and MCF10F human normal breast epithelial cells were incubated with 2.5 and 5 μM, and MDA-MB-231 human breast cancer cells with 10 and 20 μM, of either GA-TPP$^+$C$_{10}$ or PCA-TPP$^+$C$_{10}$ for 48 h. Staurosporine (STS; 10 μM) was used as a positive apoptosis-induction control. Apoptosis was assessed as annexin V-FITC positive cells using flow cytometry (FACS Canto, BD Biosciences). Representative dot plots are presented for (A) MCF7, (C) MDA-MB-231 and (E) MCF 10F. Quantification of dot plots for (B) MCF7, (D) MDA-MB-231 and (F) MCF 10F was done using the Cyflogic software (version 1.2.1.). Alive cells (black bars) were defined as annexin V negative/propidium iodide negative and apoptotic or secondary necrotic cells (white bars) as the grouping of annexin V positive/propidium iodide negative (early apoptosis) and annexin V positive/propidium iodide positive cells (late apoptosis). Control columns represent cells incubated only with vehicle and results are expressed as percentage of total cells (mean ± SEM, n = 3). *: significant difference compared to control (one way ANOVA with Bonferroni post-test; $p < 0.05$), **: $p < 0.01$, ***: $p < 0.001$.

The cell lines studied represent four of the five types of breast cancer described in patients, and they differ from each other mainly in their expression-pattern for estrogen and EGF receptors (ER and HER2/neu, respectively) (Gazdar et al., 1998; Hevir et al., 2011; Boyle, 2012). Importantly, ER and HER2/neu are known to affect mitochondrial metabolism by stimulating transcription of mitochondrial respiratory complexes, inhibiting the formation of the mitochondrial transition pore and the triggering of intrinsic apoptosis and increasing mitochondrial antioxidant defense (ER) (Chen et al., 2009; Chaudhri et al., 2012), or inhibiting mitochondrial respiration and stimulating aerobic glycolysis (HER2/neu) (Ding et al., 2012). Thus, the use of cell lines which differentially express the latter receptors allowed us to test the cytotoxic effect of our compounds in relation to different phenotypic scenarios in BC.

As shown, all five decyl-polyhydroxybenzoates-TPP$^+$ exerted a concentration-dependent cytotoxic effect on the five cell lines studied, with little differences in the effect of each compound. Although four of the

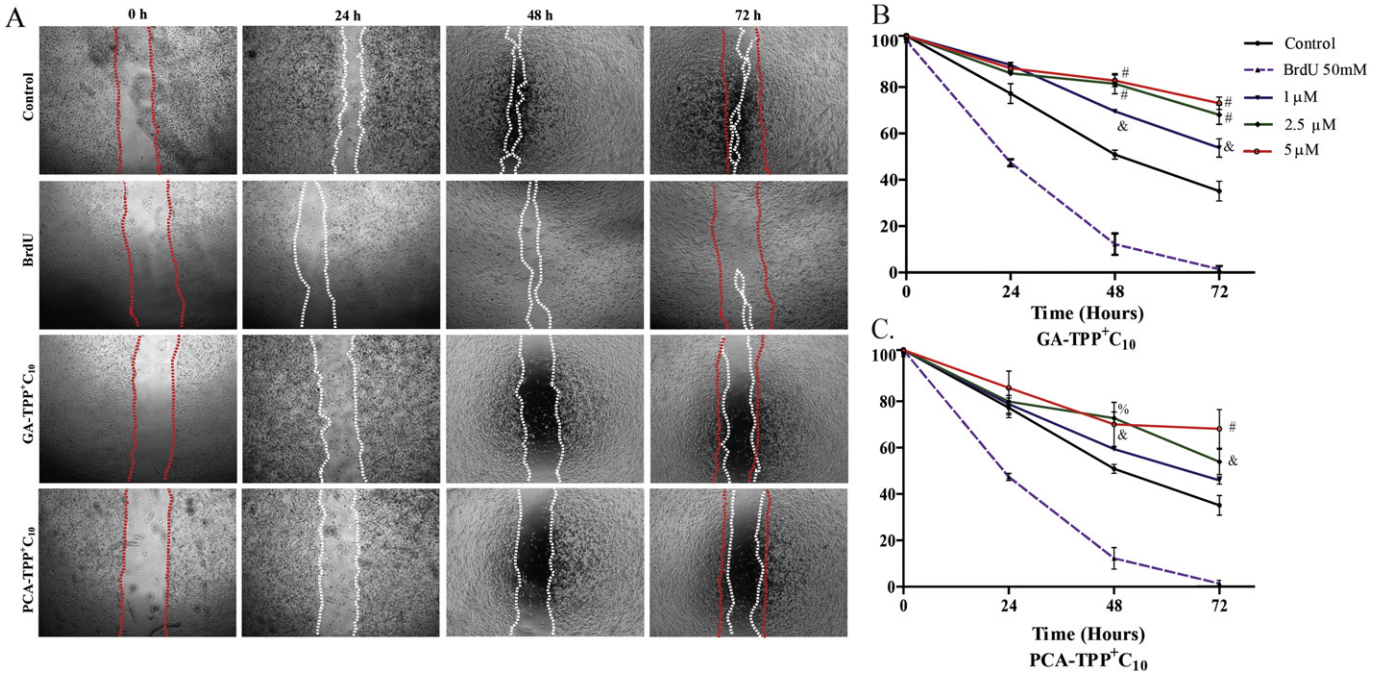

Fig. 7. Effect of decyl-polyhydroxybenzoates-TPP^+ on the migratory ability of MDA-MB-231 cells. MDA-MB-231 human breast cancer cells were grown to almost 100% confluency and the bottom of each well was wounded with a 200 μL micropipette tip (corresponding to the area between the two red lines). Afterwards, cells were incubated with increasing concentrations (1, 2.5 and 5 μM) of each TPP^+-linked polyhydroxybenzoate in a serum-free media for 72 h and photographed at 0, 24, 48 and 72 h. (A) Representative images of wounds at all the time points. DMSO in a serum-free media was used as a negative control for migration inhibition and BrdU (30 and 50 μM) in 10% FBS supplemented-media as positive migration controls. Results are expressed as percentage of original wound area at each analyzed time for (B) GA-TPP^+C_{10} or (C) PCA-TPP^+C_{10} (mean ± SEM, n = 3). %: significant difference compared to DMSO (two way ANOVA with Bonferroni post-test; $p < 0.05$), &: $p < 0.01$, #: $p < 0.001$.

cell lines seem similarly sensitive to the compounds (*i.e.*, MCF7 (ER^+-$HER2/neu^-$), AU565 (ER^--$HER2/neu^+$), BT-549 (ER^--$HER2/neu^-$) and MDA-MB-361 (ER^+-$HER2/neu^+$)), the MDA-MB-231 line (ER^--$HER2/neu^-$) appears to require slightly higher concentrations at 48 and 72 h, showing only the minor change in its IC_{50} values. This result allows us to postulate that the cytotoxic effect of the TPP^+ derivatives would be independent on the expression of either ER or HER2/neu, especially when considering that the more resistant MDA-MB-231 cell line presents the same expression pattern as the sensitive BT-549 cell line (Rhodes et al., 2015). Indeed, both belong to TNBC-subtype of cancer cells and also express markers of cancer stem cells (CSC), being referred to as CSC-like populations. Consequently, they might show intrinsic resistance to the inhibitory action of drugs on TORC1/2 (Bhola et al., 2016). Moreover, TNBC cells have been shown to possess higher mitochondrial mass (Pelicano et al., 2014), a result consistent with our finding that MDA-MB-231 are capable of significantly higher maximal oxygen consumption rates than MCF7 cells. The latter might be another reason underlying the slightly higher IC_{50} values obtained upon incubation of MDA-MB-231 cells with the five decyl-polyhydroxybenzoates-TPP^+ derivatives. Additionally, although both BT-549 and MDA-MB-231 belong to the TNBC subtype, they can be classified into different subtypes according to their expression of EGFR (Yunokawa et al., 2012). Thus, BT-549 belongs to the basal-like TNBC, with high expression of EGFR, while MDA-MB-231 cells are classified as non-basal TNBC due to their null expression of this receptor (Furuya et al., 2016). Interestingly, metabolic differences have also been found between basal-like and non-basal TNBCs, with both subtypes exhibiting a larger dependence upon glycolytic metabolism (opposite to that observed in ER or HER2/neu expressing BC) (Pelicano et al., 2014; Zhuang et al., 2014), and non-basal cancer being also able to rely on glutaminolysis for energy generation (Simpson et al., 2012). A possible explanation for the fact that TNBC cells exhibit such glycolytic-dependence while possessing a relatively higher mitochondrial mass might be an increased expression of the Complex V-inhibitor IF1, which would reduce ATP generation by mitochondria (Sanchez-Arago et al., 2013; Barbato et al., 2015; Sanchez-Cenizo et al., 2010; Sanchez-Arago et al., 2012). Therefore, it is possible that the minor differences in sensitivity to the decyl-polyhydroxybenzoates-TPP^+ observed between the two TNBC cell-lines could be related to their different metabolic profiles.

Survival experiments with control molecules (lacking either the TPP^+ or the polyhydroxybenzoate moieties) show that the non-TPP^+ compounds have no cytotoxic effect at concentrations up to 400 μM, while the molecule lacking the polyhydroxybenzoate ($C_{10}TPP^+$) moiety induces a strong cytotoxic effect on BC cells. This increased cytotoxicity might involve fatty acid cycling, which would induce a large mitochondrial-transmembrane leak of protons (Severin et al., 2010). However, cell death induced by $C_{10}TPP^+$ appears to imply a major release of LDH to the extracellular space, supporting a necrotic-like cell death mechanism, in contrast with an apparent apoptotic-like cell death induced by the TPP^+-linked polyhydroxybenzoates. Additionally, the complete absence of cytotoxic effect induced by the BA-TPP^+C_{10} molecule (Table II) indicates that the presence of hydroxyl groups in the aromatic ring is highly important for such effect, and further supports the notion that the cytotoxic action of decyl-polyhydroxybenzoates-TPP^+ would not be related to the sole presence of the TPP^+ moiety.

In addressing the possible mitochondrial mechanism underlying the cytotoxic effect of the TPP^+-derivatives, MCF7 and MDA-MB-231 cells were chosen since they represent two different metabolic states, with MCF7 showing a mixed metabolism (oxidative and glycolytic) and MDA-MB-231 a primary glycolytic metabolism with glutaminolysis activation (Pelicano et al., 2014). Rotenone-sensitive oligomycin-inhibited oxygen consumption was first used as a marker of mitochondrial respiratory activity. Results show that the addition of TPP^+-linked polyhydroxybenzoates to oligomycin-treated cells is able to increase oxygen consumption in both MCF7 and MDA-MB-231 cells. Such increase could be the result of the compounds ability to induce either a weak uncoupling of oxidative phosphorylation or an increase in

superoxide anion production at the electron transport chain (ETC) level (Mracek et al., 2014). Thus, we next assessed the effect of TPP^+-derivatives on mitochondrial superoxide anion production (Maity et al., 2009). Results show that TPP^+-linked polyhydroxybenzoates are not able to induce a major increase of superoxide anion production in concentrations up to 10–20 μM. Although a concentration of 50 μM was indeed able to induce an increase in mitochondrial superoxide anion levels, the lack of effect at lower concentrations, which already induce an increase in oxygen consumption, allows us to suggest that although it may contribute in some degree, mitochondrial superoxide anion production would not be the main responsible for the increment in oxygen consumption and the cytotoxic effect of decyl-polyhydroxybenzoates-TPP^+. As we indicated above, if mitochondrial superoxide anion production is not significantly enhanced, the increment in oxygen consumption could be related to an uncoupling of oxidative phosphorylation. Uncoupling implies that protons are being translocated from the intermembrane space into the mitochondrial matrix, therefore dissipating the proton gradient needed for ATP synthesis at the Complex V and decreasing Ψ_m (Brand and Nicholls, 2011). In order to assess the effect of our compounds on Ψ_m, we used the fluorescent probe safranin-O, which is able to accumulate rapidly, and in a transmembrane potential-dependent manner, into the mitochondria of lightly permeabilized cells, where its fluorescence is quenched. When the membrane potential is diminished the probe exits the mitochondrial compartment, and its relative fluorescence is increased (Akerman and Saris, 1976; Akerman and Wikstrom, 1976; Amora et al., 2008). Results show that all TPP^+-derivatives are able to induce a rapid and concentration-dependent loss of Ψ_m. Taken together; the previous results show that a weak uncoupling of the oxidative phosphorylation, partially accompanied by an increase in mitochondrial superoxide anion production, could be the triggering event in the cytotoxicity of TPP^+-linked polyhydroxybenzoates. Noteworthy, the compounds were able to induce a maximal uncoupling (equal to that observed after the addition of the known uncoupler CCCP) only at 20 μM (as measured by safranin-O) or 50 μM (as measured by oxygraphy). Thus, they may be considered relatively safer uncouplers, since their uncoupling effect increased only gradually as its concentration increased, thereby widening the distance between therapeutic and toxic doses (Lou et al., 2007).

One of the most important effects of a Ψ_m loss is the major inhibition of mitochondrial ATP synthesis which, if not compensated by other synthetic pathways, could lead to cell death. Thus, we investigated the effect of TPP^+-linked polyhydroxybenzoates on ATP levels, and observed that, contrary to what could be expected, no major ATP losses were induced, possibly due to the short incubation times used or to compensatory effects by other pathways such as glycolysis, fatty acid oxidation and TCA cycle (Hardie et al., 2012). In order for cells to activate the compensatory ATP-generating mechanisms, metabolic sensors must be activated upon initial signals of ATP decrease (Yuan et al., 2013). In that regard, one of the main sensors described in cancerous cells is the AMP-activated kinase (AMPK). Upon its activation, AMPK induces the activation of several ATP generating pathways, such as glycolysis, beta-oxidation and glucose uptake, and inhibits ATP-consuming macromolecule-synthetic pathways (Hardie et al., 2012). Thus, we tested the effect of the co-incubation of BC cells with TPP^+-linked polyhydroxybenzoates and the AMPK inhibitor Compound C on ATP levels. As it was shown, Compound C significantly enhanced the ATP lowering effect of our compounds, evidencing that AMPK activation might play a role in a cellular attempt of compensating an initial decrease in ATP levels induced by the uncoupling TPP^+-derivatives. Similar results were obtained when diadenylate-pentaphosphate (an adenilate kinase inhibitor) was used instead of Compound C. Adenylate kinase is one of the main activators of AMPK upon increases in the ADP/ATP ratio (Dzeja and Terzic, 2009). The co-addition of the adenylate-kinase inhibitor Ap5A together with GA-TPP^+ C_{10} or PCA-TPP^+ C_{10} resulted in a larger decrease in cellular ATP levels. Such a result further supports the concept that TPP^+-linked polyhydroxybenzoates are able to inhibit the synthesis of mitochondrial ATP, possibly through the uncoupling of oxidative phosphorylation and the dissipation of Ψ_m. It is necessary to note, however, that the effect observed in MDA-MB-231 cells was never as strong as that seen in MCF7 cells, suggesting that the former cells might possess other AMPK-independent ATP-generating compensatory mechanisms (*e.g.*, glutaminolysis) (Simpson et al., 2012; Jin et al., 2015). Interestingly, the ATP levels of normal breast epithelial MCF 10F cells were almost not affected by the compounds tested, either alone or in combination with the two mentioned inhibitors. The latter result might imply that normal epithelial cells are less significantly affected by the uncoupling effect of TPP^+-linked polyhydroxybenzoates, or that they have major ATP pathways, independent of both adenylate kinase and AMPK, to compensate for the putative decrease in ATP caused by the TPP^+-derivatives.

It is important to note that a loss of mitochondrial transmembrane potential also prevents the operation of another important mitochondrial process, the Ca^{2+} uptake into the matrix space by the Ca^{2+} uniporter activity, which it is located in the inner membrane and is directly coupled to the electron flow through respiratory chain (Kirichok et al., 2004). Therefore, when there is a loss of mitochondrial Ca^{2+} uptake, an increase in cytosolic [Ca^{2+}] leads to the activation of Ca^{2+}-dependent degradation enzymes, including phospholipases, proteases and endonucleases, which in turn causes damage to vital macromolecules and results in cell death (Dejeans et al., 2010). Cellular death might be also triggered by the release of classical intra-mitochondrial apoptosis activators such as cytochrome *c*, apoptosis-inducing factor, endonuclease G or Smac/DIABLO (Kwong et al., 2007; Sareen et al., 2007). Accordingly, MCF7 and MDA-MB-231 exhibited a characteristic annexin V-positive staining after the incubation with the TPP^+-linked polyhydroxybenzoates, while propidium iodide-exclusive staining was observed only in about 5% of the cellular population. The absence of a necrotic-like phenotype is in accordance with the low levels of LDH release exerted by GA-TPP^+ C_{10} (even at a 20 μM concentration), and it is observed despite the statistically significant increase in superoxide anion production induced by all the TPP^+-derivatives (at 20–50 μM concentrations). Although MDA-MB-231 cells show significantly less apoptotic signal, this is consistent with their slightly increased resistance to the cytotoxic effect of the TPP^+-derivatives observed in survival assays. Of note, MCF 10F cells showed very little cell death when incubated with TPP^+-derivatives for 48 h, a result that might be related to the lack of ATP-lowering effect observed before. Thus, evidence obtained with MCF 10F suggests that the cytotoxic effect of TPP^+-linked polyhydroxybenzoates might be selective for cancer cells. Nonetheless, *in vivo* experiments with animals bearing human-cell tumors are warranted to obtain further support to the latter contention.

Another important process involved in BC progression is cellular migration, as it allows cancer cells to metastasize and spread the disease to different organs. This active process is highly dependent on ATP levels, and thus might be affected by mitochondrial uncouplers (Zhou et al., 2014). Indeed, our results show that sub-lethal concentrations of TPP^+-derivatives are able to diminish the migratory capacity of MDA-MB-231 cells, already at 48 h of incubation. Although ATP decrease is one possible explanation for the inhibition induced by the TPP^+-linked polyhydroxybenzoates on cellular migration, two possible alternative mechanisms that could underlie such effect are also to be noted. The first one would involve the relation between mitochondrial dynamics and lamellipodia formation described by Zhao et al. (2013). As reported by the authors, inhibition of mitochondrial fission, or up-regulation of mitochondrial fusion, resulted in decreased mitochondrial distribution to lamellipodia, thus inhibiting migration of MDA-MB-231 cells. In fact, results from such study show that the classical uncoupler CCCP is able to completely ablate cellular migration and lamellipodia formation already after a 30 min incubation (Zhao et al., 2013). A second mechanism that could possibly underlie the migratory-inhibiting effect of our compounds might involve the ability of phenolic acids (such as protocatechuic or gallic acids) to decrease migration through the

inhibition of NF-κB and small GTPases (including Ras, Cdc42, Rac1, Rhoa and RhoB), as reported by Ho et al. (2010) and (Lin et al. (2011)) in AGS gastric adenocarcinoma cells. In view of our results, we believe that the inhibitory mechanism on cellular migration of decyl-polyhydroxybenzoates-TPP^+ warrants future research.

5. Conclusions

Taken together, our results showed that the mitochondrially-targeted decyl-polyhydroxybenzoates (namely: SA-TPP^+C_{10}, GA-TPP^+C_{10}, PIA-TPP^+C_{10}, PCA-TPP^+C_{10} and TPP^+C_{10}) are cytotoxic for all tested breast cancer cell lines, regardless their hormone or growth factor receptors (ER and HER2/neu –respectively-) expression pattern. Such cytotoxicity appears to be triggered by an initial loss of mitochondrial transmembrane potential, due to a weak uncoupling of the oxidative phosphorylation. The former event could lead, in the long term, to a mild decline in cellular ATP levels (although such decline might be partially compensated by the activation of AMPK) and to a release of mitochondrial calcium into the cytosol, among other processes, resulting in the activation of apoptotic pathways. Moreover, the decyl-polyhydroxybenzoates-TPP^+ are shown to partially inhibit the migratory ability of highly metastatic MDA-MB-231 cells at sub-lethal concentrations. Thus, we postulate that decyl-polyhydroxybenzoates-TPP^+ represent molecules which warrant further research for their potential as putative pharmacological agents in the treatment of all subtypes of breast cancer.

Conflict of interest statement

The authors declare no competing financial interest.

Author contributions

C.S-A., S.F-R., J.A.J. and J.F. designed the study. M.M-R., S.R. and V.C-C. synthesized the compounds. C.S-A., S.F-R., D.G-R. and M.P. preformed the experimental work. C.S-A., S.F-R., L.P-S., H.S., J.A.J. and J.F. analyzed and interpreted the data. C.S-A., S.F-R. and J.F. wrote the manuscript. M.C., H.S., J.D.M., E.P. and G.M.C. provided valuable administrative, technical and material support.

Transparency Document

The Transparency Document associated with this article can be found, in an online version.

Acknowledgments

We want to thank Dr. Yedi Israel for his valuable cooperation in reading and critically commenting our manuscript. This work was supported by the FONDECYT Grants 1130772 (to J.F.) and 1150090 (to H.S.), and the CONICYT PAI Grant 791220004 (to M.C.) and Ph.D. fellowship 21120872 (to C-S-A).

Appendix A. Supplementary data

Supplementary data to this article can be found online at http://dx.doi.org/10.1016/j.taap.2016.08.018.

References

Akerman, K.E., Saris, N.E., 1976. Stacking of safranine in liposomes during valinomycin-induced efflux of potassium ions. Biochim. Biophys. Acta 426 (4), 624–629.
Akerman, K.E., Wikstrom, M.K., 1976. Safranine as a probe of the mitochondrial membrane potential. FEBS Lett. 68 (2), 191–197.
Amora, D.N., et al., 2008. Mitochondrial dysfunction induced by pancreatic and crotalic (*Crotalus durissus terrificus*) phospholipases A2 on rabbit proximal tubules suspensions. Toxicon 52 (8), 852–857.
Ayub, A., Yip, W.K., Seow, H.F., 2015. Dual treatments targeting IGF-1R, PI3K, mTORC or MEK synergize to inhibit cell growth, induce apoptosis, and arrest cell cycle at G1 phase in MDA-MB-231 cell line. Biomed. Pharmacother. 75, 40–50.
Barbato, S., et al., 2015. The inhibitor protein (IF1) of the F1F0-ATPase modulates human osteosarcoma cell bioenergetics. J. Biol. Chem. 290 (10), 6338–6348.
Bhola, N.E., et al., 2016. Treatment of triple-negative breast cancer with TORC1/2 inhibitors sustains a drug-resistant and notch-dependent cancer stem cell population. Cancer Res. 76 (2), 440–452.
Boyle, P., 2012. Triple-negative breast cancer: epidemiological considerations and recommendations. Ann. Oncol. vi7–v12 23 Suppl 6.
Brand, M.D., Nicholls, D.G., 2011. Assessing mitochondrial dysfunction in cells. Biochem. J. 435 (2), 297–312.
Chaudhri, R.A., et al., 2012. Membrane estrogen signaling enhances tumorigenesis and metastatic potential of breast cancer cells via estrogen receptor-alpha36 (ERalpha36). J. Biol. Chem. 287 (10), 7169–7181.
Chen, J.Q., et al., 2009. Regulation of mitochondrial respiratory chain biogenesis by estrogens/estrogen receptors and physiological, pathological and pharmacological implications. Biochim. Biophys. Acta 1793 (10), 1540–1570.
Dejeans, N., et al., 2010. Endoplasmic reticulum calcium release potentiates the ER stress and cell death caused by an oxidative stress in MCF-7 cells. Biochem. Pharmacol. 79 (9), 1221–1230.
Ding, Y., et al., 2012. Receptor tyrosine kinase ErbB2 translocates into mitochondria and regulates cellular metabolism. Nat. Commun. 3, 1271.
Dzeja, P., Terzic, A., 2009. Adenylate kinase and AMP signaling networks: metabolic monitoring, signal communication and body energy sensing. Int. J. Mol. Sci. 10 (4), 1729–1772.
Frey, C., et al., 2007. Comparative cytotoxicity of alkyl gallates on mouse tumor cell lines and isolated rat hepatocytes. Comp. Biochem. Physiol. A Mol. Integr. Physiol. 146 (4), 520–527.
Fulda, S., Galluzzi, L., Kroemer, G., 2010. Targeting mitochondria for cancer therapy. Nat. Rev. Drug Discov. 9 (6), 447–464.
Furuya, K., et al., 2016. Eribulin upregulates miR-195 expression and downregulates Wnt3a expression in non-basal-like type of triple-negative breast cancer cell MDA-MB-231. Hum. Cell 29 (2), 76–82.
Gazdar, A.F., et al., 1998. Characterization of paired tumor and non-tumor cell lines established from patients with breast cancer. Int. J. Cancer 78 (6), 766–774.
Gomes, L.R., et al., 2015. RECK is not an independent prognostic marker for breast cancer. BMC Cancer 15, 660.
Hardie, D.G., Ross, F.A., Hawley, S.A., 2012. AMPK: a nutrient and energy sensor that maintains energy homeostasis. Nat. Rev. Mol. Cell Biol. 13 (4), 251–262.
Hevir, N., et al., 2011. Expression of estrogen and progesterone receptors and estrogen metabolizing enzymes in different breast cancer cell lines. Chem. Biol. Interact. 191 (1–3), 206–216.
Ho, H.H., et al., 2010. Anti-metastasis effects of gallic acid on gastric cancer cells involves inhibition of NF-kappaB activity and downregulation of PI3K/AKT/small GTPase signals. Food Chem. Toxicol. 48 (8–9), 2508–2516.
What is breast cancer? Available from http://www.cancer.org/cancer/breastcancer/detailedguide/breast-cancer-what-is-breast-cancer
Jara, J.A., et al., 2014. Antiproliferative and uncoupling effects of delocalized, lipophilic, cationic gallic acid derivatives on cancer cell lines. Validation in vivo in singenic mice. J. Med. Chem. 57 (6), 2440–2454.
Jin, L., Alesi, G.N., Kang, S., 2015. Glutaminolysis as a target for cancer therapy. Oncogene.
Kirichok, Y., Krapivinsky, G., Clapham, D.E., 2004. The mitochondrial calcium uniporter is a highly selective ion channel. Nature 427 (6972), 360–364.
Kurebayashi, N., Kodama, T., Ogawa, Y., 1980. P1,P5-Di(adenosine-5′)pentaphosphate(Ap5A) as an inhibitor of adenylate kinase in studies of fragmented sarcoplasmic reticulum from bullfrog skeletal muscle. J. Biochem. 88 (3), 871–876.
Kwong, J.Q., et al., 2007. The mitochondrial respiratory chain is a modulator of apoptosis. J. Cell Biol. 179 (6), 1163–1177.
Lamb, R., et al., 2015. Antibiotics that target mitochondria effectively eradicate cancer stem cells, across multiple tumor types: treating cancer like an infectious disease. Oncotarget 6 (7), 4569–4584.
Lin, H.H., et al., 2011. Protocatechuic acid inhibits cancer cell metastasis involving the down-regulation of Ras/Akt/NF-kappaB pathway and MMP-2 production by targeting RhoB activation. Br. J. Pharmacol. 162 (1), 237–254.
Lou, P.H., et al., 2007. Mitochondrial uncouplers with an extraordinary dynamic range. Biochem. J. 407 (1), 129–140.
Ma, T., et al., 2014. Inhibition of AMP-activated protein kinase signaling alleviates impairments in hippocampal synaptic plasticity induced by amyloid beta. J. Neurosci. 34 (36), 12230–12238.
Madak, J.T., Neamati, N., 2015. Membrane permeable lipophilic cations as mitochondrial directing groups. Curr. Top. Med. Chem. 15 (8), 745–766.
Maity, P., et al., 2009. Indomethacin, a non-steroidal anti-inflammatory drug, develops gastropathy by inducing reactive oxygen species-mediated mitochondrial pathology and associated apoptosis in gastric mucosa: a novel role of mitochondrial aconitase oxidation. J. Biol. Chem. 284 (5), 3058–3068.
Maiuri, M.C., Kroemer, G., 2015. Essential role for oxidative phosphorylation in cancer progression. Cell Metab. 21 (1), 11–12.
Modica-Napolitano, J.S., Aprille, J.R., 2001. Delocalized lipophilic cations selectively target the mitochondria of carcinoma cells. Adv. Drug Deliv. Rev. 49 (1–2), 63–70.
Mracek, T., et al., 2014. ROS generation and multiple forms of mammalian mitochondrial glycerol-3-phosphate dehydrogenase. Biochim. Biophys. Acta 1837 (1), 98–111.
Murphy, M.P., Smith, R.A., 2007. Targeting antioxidants to mitochondria by conjugation to lipophilic cations. Annu. Rev. Pharmacol. Toxicol. 47, 629–656.

Neuzil, J., et al., 2013. Classification of mitocans, anti-cancer drugs acting on mitochondria. Mitochondrion 13 (3), 199–208.
Pelicano, H., et al., 2014. Mitochondrial dysfunction in some triple-negative breast cancer cell lines: role of mTOR pathway and therapeutic potential. Breast Cancer Res. 16 (5), 434.
Ralph, S.J., et al., 2010. The causes of cancer revisited: "mitochondrial malignancy" and ROS-induced oncogenic transformation - why mitochondria are targets for cancer therapy. Mol. Asp. Med. 31 (2), 145–170.
Rhodes, L.V., et al., 2015. Regulation of triple-negative breast cancer cell metastasis by the tumor-suppressor liver kinase B1. Oncogenesis 4, e168.
Sanchez-Arago, M., et al., 2012. IF1 reprograms energy metabolism and signals the oncogenic phenotype in cancer. Cell Cycle 11 (16), 2963–2964.
Sanchez-Arago, M., et al., 2013. Expression, regulation and clinical relevance of the ATPase inhibitory factor 1 in human cancers. Oncogenesis 2, e46.
Sanchez-Cenizo, L., et al., 2010. Up-regulation of the ATPase inhibitory factor 1 (IF1) of the mitochondrial H^+-ATP synthase in human tumors mediates the metabolic shift of cancer cells to a Warburg phenotype. J. Biol. Chem. 285 (33), 25308–25313.
Sareen, D., et al., 2007. Mitochondria, calcium, and calpain are key mediators of resveratrol-induced apoptosis in breast cancer. Mol. Pharmacol. 72 (6), 1466–1475.
Severin, F.F., et al., 2010. Penetrating cation/fatty acid anion pair as a mitochondria-targeted protonophore. Proc. Natl. Acad. Sci. U. S. A. 107 (2), 663–668.
Simpson, N.E., et al., 2012. An in vitro investigation of metabolically sensitive biomarkers in breast cancer progression. Breast Cancer Res. Treat. 133 (3), 959–968.
Breast Cancer Epidemiology. 2010: Springer-Verlag New York. XIII, 417.
Tan, A.S., et al., 2015. Mitochondrial genome acquisition restores respiratory function and tumorigenic potential of cancer cells without mitochondrial DNA. Cell Metab. 21 (1), 81–94.
Viale, A., Corti, D., Draetta, G.F., 2015. Tumors and mitochondrial respiration: a neglected connection. Cancer Res. 75 (18), 3685–3686.
Villanueva, M.T., 2015. Metabolism: the mitochondria thief. Nat. Rev. Cancer 15 (2), 70.
Yan, B., Dong, L., Neuzil, J., 2015. Mitochondria: an intriguing target for killing tumour-initiating cells. Mitochondrion 26, 86–93.
Yuan, H.X., Xiong, Y., Guan, K.L., 2013. Nutrient sensing, metabolism, and cell growth control. Mol. Cell 49 (3), 379–387.
Yunokawa, M., et al., 2012. Efficacy of everolimus, a novel mTOR inhibitor, against basal-like triple-negative breast cancer cells. Cancer Sci. 103 (9), 1665–1671.
Zhao, J., et al., 2013. Mitochondrial dynamics regulates migration and invasion of breast cancer cells. Oncogene 32 (40), 4814–4824.
Zhou, H., et al., 2014. The inhibition of migration and invasion of cancer cells by graphene via the impairment of mitochondrial respiration. Biomaterials 35 (5), 1597–1607.
Zhuang, Y., et al., 2014. Mechanisms by which low glucose enhances the cytotoxicity of metformin to cancer cells both in vitro and in vivo. PLoS One 9 (9), e108444.